Carbohydrate Polymers 87 (2012) 658–666

Contents lists available at SciVerse ScienceDirect

Carbohydrate Polymers

journal homepage: www.elsevier.com/locate/carbpol

Influence of native starch's properties on starch nanocrystals thermal properties

Déborah LeCorre, Julien Bras, Alain Dufresne*

The International School of Paper, Print Media and Biomaterials (Pagora), Grenoble Institute of Technology, BP 65 – F-38402 Saint Martin d'Hères Cedex, France

ARTICLE INFO

Article history:
Received 29 June 2011
Received in revised form 14 August 2011
Accepted 17 August 2011
Available online 24 August 2011

Keywords:
Starch
Nanocrystals
Botanic origin
Amylose
Thermal properties

ABSTRACT

Starch nanocrystals (SNC) are crystalline square-like platelet about 10 nm thick and 50–100 nm equivalent diameters. Depending on the botanic origin of starch these platelets show different features. The aim of the present study was (i) to assess the thermal stability of SNC in different processing conditions (i.e., excess water and dry) and (ii) to investigate the potential influence of botanic origin on thermal stability. The thermal properties of five types of starches (waxy maize, normal maize, high amylose maize, potato and wheat) and their corresponding SNC were characterized by differential scanning calorimetry (DSC) and thermogravimetric analysis (TGA). SNC revealed two endothermic transitions. No correlation between melting temperature and botanic origin was found. However, a review of starch thermal properties allowed to postulate for the mechanism involved in SNC thermal transitions. It was also found that SNC can be used in wet processes below 100 °C and in dry processes below 150–200 °C to avoid melting.

1. Introduction

In material science, researchers are looking for more and more efficient renewable materials in order to face petroleum shortage and environmental concerns. Starch is one of the most abundant materials produced by nature and this polysaccharide has already found numerous industrial applications. It is a multi-scale structure consisting of concentric alternating amorphous and crystalline lamellae. It is made of mainly two structurally distinct α-D-glucan components: amylose which is linear and amylopectin which is highly branched. Each polymer constitutes a family with differences in size, fine structure and function (Biliaderis, 2009). It is believed that the crystalline region is created by the interwining of amylopectin side-chains (Oates, 1997). Amylose molecules are thought to occur in the granule as individual molecules, randomly interspersed among amylopectin molecules. Depending on the botanic origin of starch, amylose is preferably found in the amorphous region (e.g., wheat starch) (Blanshard, 1987), interspersed among amylopectin clusters in both the amorphous and crystalline regions (e.g., normal maize starch) (Kasemsuwan & Jane, 1994), in bundles between amylopectin clusters (Blanshard, 1987), or co-crystallized with amylopectin chains (e.g., potato starch) (Blanshard, 1987). Amylose content should therefore considerably influence the crystalline organization. Depending on their X-ray diffraction pattern, reflecting long-range ordering in the granule, starches are categorized in three crystalline types (polymorphs) called A, B and C. However, a property common to most starches is gelatinization. It refers to the collapse (disruption) of molecular order (breaking of H-bonds) within the granule, along with all concomitant and irreversible changes in properties such as water uptake, granular swelling, crystallite melting, birefringence loss, starch solubilization and viscosity development (Biliaderis, 2009). It is now widely accepted that it can be view as a melting process which can be evidenced as an endothermic thermal transition in DSC measurements. Depending on the application, this property is sought for or not.

Carbohydrate chemists have developed products that have greatly expanded starch use and utility (Whistler & BeMiller, 2009). Most recent developed products from starch chemistry include starch derivatives (Ma, Chang, Yu, & Stumborg, 2009; Salam, Pawlak, Venditti, & El-tahlawy, 2010) and starch nanocrystals (SNC). SNC are crystalline platelets obtained by the acid hydrolysis of amorphous parts of starch. They are believed to correspond the starch granule's crystallites. The aim of a previous study (LeCorre, Bras, & Dufresne, unpublished results) was to assess if starch from any source could indifferently be used to prepare SNC, and if amylose content and/or botanic origin's influence on SNC's final properties. Results showed that for the same amylose content maize, potato and wheat starches resulted in rather similar size and crystallinity of SNC proving the limited impact of the botanic origin. For the same botanic origin (maize), differences in size were more important indicating the strong influence of the amylopectin content and molecular structure. Particles tended to show square-like morphology with increasing initial amylopectin content and A-type crystallinity (and thus shorter chain length). Also, it was shown by X-ray diffraction measurement that although SNC's crystallinity was higher than that of their corresponding native starches, SNC were not fully crystalline.

* Corresponding author.
E-mail address: Alain.Dufresne@pagora.grenoble-inp.fr (A. Dufresne).

0144-8617/$ – see front matter © 2011 Elsevier Ltd. All rights reserved.
doi:10.1016/j.carbpol.2011.08.042

Current potential application for SNC is bio-nano-composites. They are added as nano-fillers in a polymeric matrix to improve its mechanical and/or barrier properties as described elsewhere (LeCorre, Bras, & Dufresne, 2010; Lin, Huang, Chang, Anderson, & Yu, 2011). Most work has been oriented towards the use of new environmentally friendly polymers such as non vulcanized natural rubber (Angellier, Molina-Boisseau, & Dufresne, 2005; Angellier, Molina-Boisseau, Lebrun, & Dufresne, 2005), waterborne polyurethane (WPU also called organic solvent free polyurethane) (Chen, Wei et al., 2008), waxy maize starch (Angellier, Molina-Boisseau, Dole, & Dufresne, 2006; Viguié, Molina-Boisseau, & Dufresne, 2007), cassava starch (Garcia, Ribba, Dufresne, Aranguren, & Goyanes, 2009), pullulan (obtained by starch fermentation) (Kristo & Biliaderis, 2007), PLA (Yu et al., 2008), polyvinyl alcohol (PVA) (Chen, Cao, Chang, & Huneault, 2008) and soy protein isolate (SPI) (Zheng, Ai, Chang, Huang, & Dufresne, 2009). Although early work (Angellier, Putaux, Molina-Boisseau, Dupeyre, & Dufresne, 2005; Dufresne & Cavaillé, 1998) reported composite preparation by hot pressing, since 2006 authors have opted for a simpler casting-evaporation method at 40 °C for 24 h. The hot-pressing process consisted in first mixing freeze-dried SNC with a copolymer of styrene and butyl acrylate in latex form and heating the mixture at 90 °C for 10 min. It was then hot-pressed during 1 min under 2 MPa (300 psi) pressure to obtain films about 1 mm thick (Angellier, Putaux et al., 2005). However, this process raises the question of the potential melting of SNC. Similar issue should be considered if classical polymer processing methods, e.g., extrusion or injection molding is used. With the casting process, it was necessary to decrease the temperature of the polymer matrix before adding waxy maize SNC to avoid melting (Angellier et al., 2006). However, other authors (Garcia et al., 2009) report casting-evaporation at 50 °C after constant stirring of SNC in thermoplastic starch at 90 °C for half an hour. Most recently, compression molding was used to prepare glycerol-plasticized starch nanocrystals composites at 120 °C from a freeze-dried powder (Zheng et al., 2009). One could wonder if starchy nanoparticles are still crystalline after this treatment.

The aim of the present study is two-fold. First, it aims at assessing the maximum processing temperature for SNC in the dry state and in excess water. Second, it intends to assess the influence of using different native starches, with different botanic origin, amylose content and crystalline type, on the thermal properties of resulting SNC.

2. Experiment

2.1. Materials

Native starch granules were kindly provided by Cargill (Krefeld, Germany) according to requirements: waxy maize starch (C☆Gel 04201, 98% amylopectin), normal maize starch (Cerestar RG 03453), amylomaize (Amylogel 03003, 65–75% amylose), potato starch (C☆Gel 30002) and wheat starch (Cerestar PT 20002). Sulfuric acid (96–99%, Sigma Aldrich) was used after dilution at 3.16 M with distilled water.

2.2. Preparation of starch nanocrystals

The same optimized hydrolysis process developed by Angellier, Choisnard, Molina-Boisseau, Ozil, and Dufresne (2004) was modified and used for preparing SNC from the five different starches. Briefly, 147 g of native starch was mixed with 1 L of previously prepared diluted sulfuric acid (3 M). The suspension was kept under 400 rpm mechanical stirring at 40 °C, using a silicon oil bath, for 5 days. The final suspensions were washed by successive centrifugations in distilled water until reaching neutral pH and redispersed using Ultra Turrax for 5 min at 13,000 rpm to avoid aggregates. The obtained suspensions were filtered on a filter tissue (40 μm, ref. 03-41/31 Buisine, France). Sodium azide was added to the suspensions before storage at 4 °C to avoid microbial growth.

2.3. Microscopies

An environmental scanning electron microscope (ESEM) on a Quanta 200 FEI device (Everhart-Thornley Detector) was used at high voltage (10 kV) to confirm the morphology of native starches. Native starches were simply deposited onto carbon tape before observation.

SNC' mean size and morphology were studied using a Zeiss Ultra 55 Field Emission Gun Scanning Electron Microscope (FEGSEM). A thin Au–Pd conductive coating (~1 nm) was deposited to reduce charge effect. The samples were observed and imaged at a 6-mm working distance and 10-kV accelerating voltage. These conditions illustrate the best compromise in terms of SNC contrast and residual charge effect. In order to obtain the best possible resolution, the secondary electron imaging mode with the In-lens detector was used. The average diameter was determined using digital image analyses (ImageJ). Image analysis allows measuring the surface area of SNC. From this area, an equivalent diameter was calculated with the approximation that SNC are disc-like particles. Between 70 and 500 measurements were carried out depending on the source to determine the average diameter and standard deviation.

Atomic Force Microscopy measurements were performed on a Multimodal AFM (DI, Veeco, Instrumentation Group) with both tapping and conductive mode (C-AFM). The tips were Multi130 for tapping and MESP for C-AFM. A drop of SNC suspension was deposited on a mica substrate (split with adhesive tape) and dried for a few minutes at 40 °C. Between 30 and 110 measurements were used depending on the source to determine the average thickness and standard deviation.

2.4. Differential scanning calorimetry (DSC)

Differential scanning calorimetry measurements were done with DSC Q100 (TA Instruments, NewCastle) filled with a manual liquid nitrogen cooling system. Freeze-dried SNC powder, conditioned at 50% relative humidity (RH), was placed in a hermetically sealed pan. For samples in excess water (water content – WC = 70 wt%), the amount of water necessary to reach a 30:70 starch/H_2O ratio was directly added to the pan using a micropipette, to avoid inhomogeneous withdrawals. The sealed pans were set aside for 1 day to equilibrate. Each sample was heated from 20 °C to 120 °C when in excess water and to 260 °C when dried with a heating rate of 10 °C min^{-1}. Measurements were done in triplicate to ensure repeatability. The sample weight was between 6 and 10 mg.

2.5. Thermogravimetric analysis (TGA)

Thermogravimetric analysis (STA 6000, Perkin Elmer Instruments model, USA) was carried out to determine the thermal stability of samples under oxygen flow of 20 mL min^{-1}. The samples were heated from 30 °C to 600 °C with a heating rate of 10 °C min^{-1}. The sample weight was plotted as a function of temperature for all samples.

3. Results and discussion

3.1. Starch nanocrystals features

The influence of botanic origin, amylose content and crystalline type on the morphology of SNC has been very recently studied by

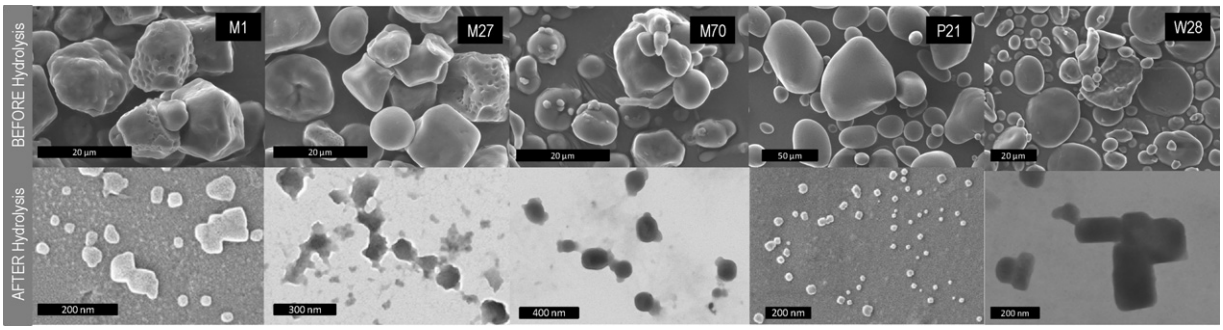

Fig. 1. Micrograph of native starches and corresponding SNC.

our group (LeCorre et al., unpublished results). The main conclusion was that the botanic origin of starch shows only a moderate influence on final properties whereas amylose content and crystalline type would be more of influence. Differences in size were rather moderate whereas differences were more pronounced when comparing shapes and crystallinity. Fig. 1 shows SEM and FEG–SEM micrographs obtained for the native starches used in this study and their corresponding SNC. Features of native starches and ensuing SNC used in this study are presented in Table 1. All SNC exhibit a platelet-like morphology with thickness 5–8 nm (Table 1). Therefore, although platelet with square-like shape should be preferred for barrier properties, all SNC can be considered as potential fillers in nanocomposites.

3.2. Thermal behavior of starches and their corresponding SNC

SNC and corresponding native starches' thermal behavior were studied both in excess water (70% WC), to simulate use in aqueous suspension such as coating or water-based composite processing, and freeze-dried (0% WC) to assess processability in "dry processes" such as extrusion. Typical responses are presented in Fig. 2a in excess water and Fig. 2b in dry state. SNC and starch granules show completely different thermograms with different number, intensity and temperature of thermal transitions. Before comparing them, it is important to understand the thermal behavior of each kind of particles, i.e., starch granules and SNC.

3.2.1. Thermal behavior of native starches

The characteristic temperatures observed for the endothermic transitions of the 5 native starches in excess water (70%) are reported in Table 2. As expected, only one endothermic peak was observed.

Data for dried samples conditioned at 50% RH are reported in Table 3. Our measurements seem to be in agreement with the latter described models as for all dry native starches only one endothermic peak was observed. For dry native starches (0% WC), the maximum of the endothermic peak ranged between 120 and 150 °C (Table 3). This temperature range is below expectations as the theoretical melting point of perfect crystallites without water is estimated at 160–210 °C (Colonna & Buleon, 2010). This might be due to the presence of residual moisture in our samples. Several authors also reported anhydrous melting point of starches by linear extrapolation of experimental data (Barron, 1999). For a given botanic origin, the temperature can also differ by up to 50 °C (Barron, 1999). In our study, no influence of the source, amylose content or crystalline type alone was observed. Indeed, starch's heat–moisture induced structural transformations (gelatinization) seem to depend rather on the interconnected factors that are its botanic source, its component molecules (amylose, amylopectin, intermediate material and minor components) content, its components molecular structure and organization, and its crystalline type". The thermal properties of starch granules have been widely investigated (Atichokudomchai, Varavinit, & Chinachoti, 2002; Barron, 1999; Biliaderis, Page, Maurice, & Juliano, 1986; Colonna & Buleon, 2010; Cooke & Gidley, 1992; Randzio, Flis-Kabulska, & Grolier, 2002; Waigh, Gidley, Komanshek, & Donald, 2000; Zhong & Sun, 2005) and have been shown to be strongly dependent on the water content. In excess water, an increase in temperature leads to the appearance of an endothermic peak (around 50–80 °C) linked to the gelatinization of starch. At intermediate water content (30–60%), the first peak is shifted up in temperature, and a higher temperature second peak is observed. At very low water content (<20%), only the higher temperature peak is observed.

Several explanations have been developed to explain the two peaks generally observed (and referred to as M1 and M2).

First, it was suggested (Donovan, 1979) that in excess water, the amorphous growth ring absorbs water and expands. As they are cross-linked by the amorphous backbone, the semi-crystalline lamellae are disrupted causing a loss of order and crystallinity (first peak M1). When the amount of water becomes insufficient to fully swell the granule, the remaining crystallites melt at higher temperature (leading to the second peak M2). An alternative explanation (Evans & Haisman, 1982) attributes the first peak (M1) to the melting of least stable crystallites which upon melting absorb all remaining water. Thus the second peak (M2) reflects the melting at higher temperatures of remaining crystallites. However, this hypothesis did not take into account possible reorganization

Table 1
Main features of native starches, and diameter and thickness of corresponding SNC.

Botanic origin	Referred to as	Granular size (µm)	Amylose (%)[a]	Crystalline type	SNC diameter		SNC thickness	
					(nm)	Counts	(nm)	Counts
High amylose maize	M70	5–20	65–75	B	118 ± 53	190	5 ± 1.6[a]	76
Normal maize	M27	5–20	27	A	58 ± 36	576	8.3 ± 3.1[a]	112
Waxy maize	M1	5–20	1	A	47 ± 42	71	6.1 ± 1.9[b]	14
Wheat	W28	2–30	28	A	100 ± 50	71	3.7 ± 0.6[c]	30
Potato	P21	5–80	21	B	52 ± 4	951	7.6 ± 1.6[a]	31

[a] Personnal measurements using Gwyddon.
[b] Conducted at SMPC, Mons, Belgium.
[c] Personnal measurements on AFM software.

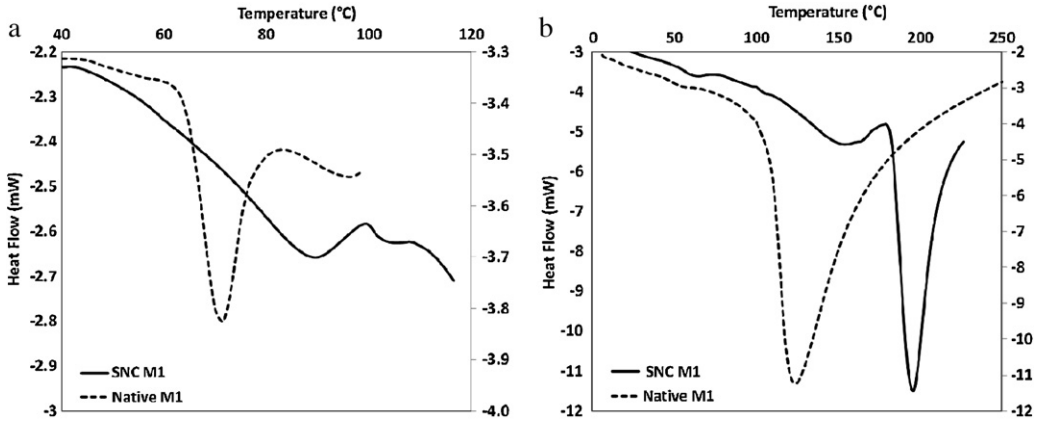

Fig. 2. DSC thermograms for native and SNC from M1 (a) in excess water and (b) in the dry state (0% WC, 50% RH conditioning).

of polymer chains in the amorphous phase and the remaining crystallites during DSC heating (Biliaderis et al., 1986). Biliaderis, Page, Slade, and Sirett (1985) suggested that the multiple melting transition profile was due to partial melting (M1) followed by recrystallization and final melting (M2). Barron suggested that it was rather linked to the heterogeneous repartition of water in starch (Barron, 1999). Zhong and Sun (2005) attributed them to the melting of crystallites and amylose lipid complexes, respectively.

Another approach to the understanding of starch thermal behavior consists in considering it from a classic polymeric point of view, as a semi-crystalline polymer whose specific heat-temperature curves exhibit the characteristics of both amorphous and crystalline polymers (Biliaderis et al., 1986). As for more classic polymers, Biliaderis et al. (1986) revealed that regardless of the water content, the melting point (T_m) is T_g-dependent in that a previous softening (relaxation) of the amorphous parts is required before crystallites can melt. As such, the melting temperature of starch crystallites is also affected by plasticizers such as water. However, despite good correlation between experimental data and the two-phase Flory Huggins model at intermediate and low water content, a three-phase model was proposed. It consisted in (i) a bulk amorphous region responsible for T_g, (ii) a non-ordered intercrystalline phase which mobility is restricted by crystallinity-induced cross-linking, and (iii) a fully ordered crystalline phase with T_g (mobile amorphous) < T_g (rigid amorphous) < T_m(rigid crystalline).

More recently, other authors (Waigh, Gidley et al., 2000; Waigh, Kato et al., 2000) proposed a liquid–crystal approach to explain the gelatinization of starch. Considering the side chain liquid crystal polymer (SCLCP) nature of amylopectin, they described a first thermal transition corresponding to a smectic (lamellar order)/nematic (orientationally ordered) transition for B-type starches, and to a nematic/isotropic phase transition for A-type starches (i.e., helix–helix dissociation) (Atichokudomchai et al., 2002; Waigh, Gidley et al., 2000). They also postulated a second transition attributed to an helix-coil transition (i.e., unwinding of double helices to a gel phase). In excess water (>60%), the difference between the two endotherms is immeasurably small for natives starches and are thought to occur almost simultaneously. At intermediate water content (30–60%), the two endotherms can be evidenced one after the other. At low water content (<30%), a direct crystalline-to-gel transition occurs as the helices unwind and only one peak is observed.

3.2.2. Thermal behavior of SNC

Based on starch analysis and proposed models, the thermal behavior of SNCs has been characterized and deeply analyzed to postulate mechanisms. The characteristic temperatures of the thermal transitions of SNC immersed in water and in the dry state are reported in Tables 2 and 3, respectively. Two observations can be made: (i) two endothermic peaks can be observed in excess water content as well as in the dry state, and (ii) a clear shift up in temperatures is observed compared to native starch granules.

Reports on the thermal behavior of SNC is scarce in literature with, up to our knowledge, only two studies (Angellier, 2005; Thielemans, Belgacem, & Dufresne, 2006). Thermal behavior data for freeze-dried waxy maize SNC was reported by Angellier (2005) to observe the plasticizing influence of water, and by Thielemans et al. (2006) to compare with grafted SNC. The first author (Angellier, 2005) reported the existence of two endothermal peaks in excess water with a broad temperature range, and the disappearance of the first peak in the dry state. The other authors (Thielemans et al., 2006) presented a DSC thermogram for waxy maize SNC in dry conditions for comparison and evidencing of grafting. The thermogram for freeze-dried SNC also showed two endothermic peaks. The first maximum peak is located around 150 °C and the second one around 200 °C. No explanation for these two peaks in the dry state could be found in the literature. Also, no data was found concerning SNC from other sources. The peak temperatures for the first peak in excess water are much higher than that reported by Angellier (2005) for waxy maize SNC. This could be attributed to an inhomogeneous water repartition (Barron, 1999) among SNC in the DSC pan. However, in the dry state, data are comparable to that of Thielemans et al. (2006). Angellier (2005) attributed this first peak to the "gelatinization" of the nanocrystals and the shift up in temperature to the crystalline nature of SNC. The broadening of the peak was attributed to the heterogeneity of waxy SNC. At 20% WC, the disappearance of this peak was reported.

Considering a classic polymeric approach (and the fact that melting temperature (T_m) is T_g-dependent), several factors could increase the melting temperature of the semi-crystalline polymer, such as (i) an increase in crystallinity, (ii) a more perfect crystals or (iii) a decrease in plasticizer content. In the case of SNC, all explanations are equally possible to explain the shift up in temperature for the first peak. Indeed, it has been demonstrated that SNC are more crystalline than their native counterparts (LeCorre et al., unpublished results). Also, due to freeze-drying, it is possible that SNC, or at least the crystalline parts of SNC, are more tightly packed and bonded via hydrogen bonds forming more perfect crystals. Finally, it has been suggested that amylose acts as a plasticizer (dilutant (Tester & Morrison, 1990)) in the starch granule. After hydrolysis, most of the amorphous starch has been hydrolyzed limiting its effect as plasticizer. Indeed, very recently, the increase in amylopectin content when hydrolyzing starch into SNC, and thus the decrease in amylose "plasticizer" content, has been confirmed (LeCorre et al., unpublished results). If no amorphous starch is left

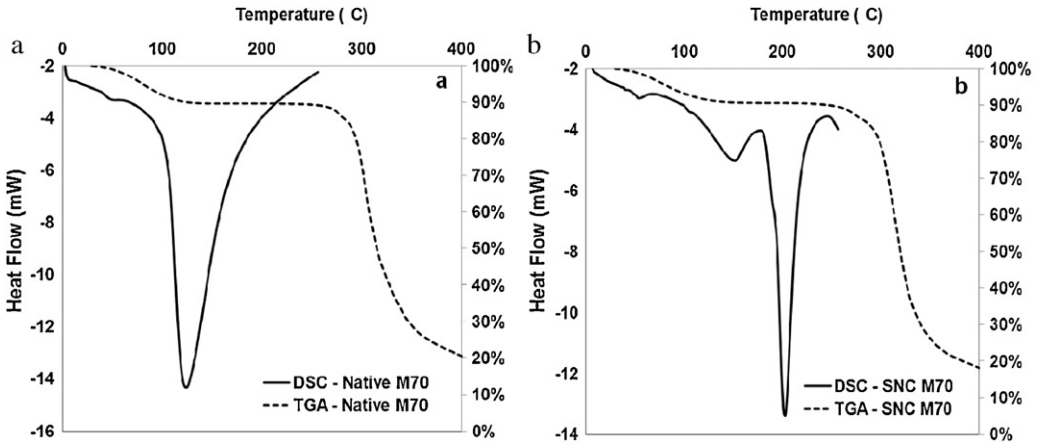

Fig. 3. DSC and TGA curves for dry (0% WC, 50% RH) (a) native M70 and (b) M70SNC.

then no more T_g can be evidenced and T_m should be high. However, it is most likely that some amorphous starch is still present leading to increased T_g and thus T_m. In excess water, the water can penetrate SNC and lower their thermal transitions compared to dry SNC.

Under the SCLCP approach, the first peak could be attributed to the smectic–nematic transition. However, with the hydrolysis of the backbone and possibly the flexible spacers of amylopectin, it takes more energy to disassociate and displace the double helixes from their lamellar organization (smectic) to nematic or isotropic state. Water facilitates this transition, explaining the lower temperatures observed in excess water.

In excess water, the second peak maximum temperatures are smaller (103–107 °C) (Table 2) than that reported by Angellier (2005) (140–160 °C). Angellier (2005) demonstrated with mass spectroscopy, that SNC heated up in excess water (80%) and above 110 °C had reduced DP. They concluded that the second peak reflected a heat-induced depolymerization rather than melting. However, no TGA data was available to confirm. Literature for cellulose nanocrystals (George, Ramana, Bawa, & Siddaramaiah, 2011; Roman & Winter, 2004; Wang, Ding, & Cheng, 2007) reported similar lower decomposition temperature for nanocrystals compared to micro-crystalline cellulose. It was attributed to the small size of the particles, the high specific surface area and thus to the outer surface structure including the presence of sulfate groups (Wang et al., 2007), also found on SNC ((Angellier, 2005) and confirmed by elemental analysis not presented here). The neutralization of these sulfate groups shifted the degradation to higher temperatures.

However, under the SCLCP approach, the second peak should rather be attributed to further melting (i.e., to the helix-coil transition). This is why the thermal degradation process is detailed latter in this study.

In dry conditions, data for waxy maize SNC was in agreement with those reported by Thielemans et al. (2006)with a very high second peak maximum temperature of about 200 °C. The presence of two endothermic peak could be attributed, as it is the case for granular starch according to Evans and Haisman (1982), to the presence of weak crystallites (least stable) that melt first (M1 peak) and of more stable crystallites that melt at higher temperature (M2 peak).

Combining the polymeric approach and the SCLCP model, the observed melting transitions could be explained as such. On the one hand, when the experiment starts in excess water, the first peak should be attributed to the helix–helix dissociation (smectic/nematic or isotropic transition) and the second one, which happens right after (only 20 °C later), to the unwinding of the helixes (helix-coil transition), which agrees with the interpretation given by Biliaderis, Mazza, and Przybylski (1993) and Tester and Morrison (1992) to the melting transitions M1 and M2 observed for granular starch.

On the other hand, when the experiment starts from the dry state, the two peaks could be attributed to the direct transition from smectic to coil (gel state), as reported by Waigh, Gidley et al. (2000) for starch at low water content of two types of crystallites. Thus, the first peak (corresponding to the M1 peak of native starches according to Evans and Haisman (1982)) could be attributed to the melting of least stable crystallites, and the second one (corresponding to M2) to the more stable remaining crystallites. Especially since the temperature range observed for SNC peaks corresponds to the theoretical melting temperature of crystallites (168–257 °C)(Barron, 1999) as mentioned earlier. To confirm this postulated mechanisms, it was important to prove that no degradation or depolymerization occurred in these conditions.

3.3. Thermal degradation of starches and ensuing SNC

To assess the possibility that the second endothermal peak in dry conditions corresponds to the melting of the crystallites, TGA measurements were carried out for the five different starch sources and freeze-dried SNC used for DSC measurements. Typical superimposed DSC and TGA curves for native starch and SNC are presented in Fig. 3. For native starches, the mechanism is confirmed with degradation at temperatures much higher (about 300 °C) than the endothermic peaks (about 120–150 °C). Similar results were obtained whatever the starch source. Concerning SNC, it seems that the two endothermic transitions observed in DSC measurements occur before the thermal degradation observed in TGA. Even if initial water evaporation is observed with TGA for freeze-dried SNC, no early stage depolymerization is observed. The degradation temperature of SNC is higher than the temperature of the second DSC peak, whatever the source of starch. This confirms that (i) the second endotherm reflects the melting of the crystallites (as extrapolated from calculations) (Barron, 1999) and that (ii) SNC correspond to starch crystallites described in literature.

It should also be noted, from TGA results presented in Fig. 4, that slight differences between native starches and SNC can be observed. Indeed, SNC depolymerization starts earlier than for native starch. This is attributed to the presence of sulfate groups at the surface of SNC (Angellier, 2005) which catalyze the reaction as explained earlier. At 200–300 °C, the sulfonic acid groups are thermally decompose (Jiang, Yao, McKinney, & Wilkie, 1999) and thus the depolymerization rate slows down. The final weigh is found to be identical. This phenomenon was also observed when comparing cellulose nanocrystals and MCC (microcrystalline

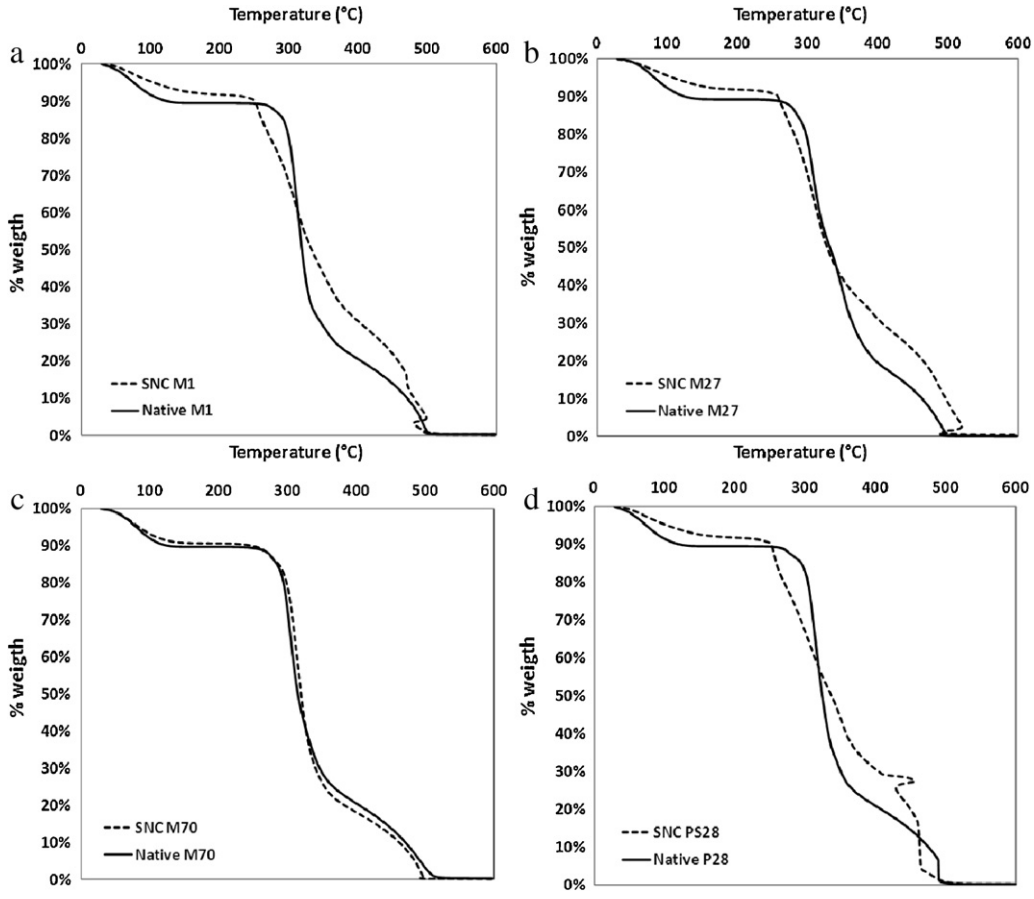

Fig. 4. Comparison between TGA curves of native starch and SNC for (a) M1, (b) M27, (c) M70 and (d) PS28.

cellulose) with comparable acid sulfate content (Wang et al., 2007). This difference is not observed for M70 SNC as particles are bigger (Table 1), and thus the specific surface area is smaller and less sulfate groups can catalyze the reaction. The higher the initial amylose content, the bigger the SNC and the higher the degradation temperature and the more similar to the initial starch's thermal behavior (as less sulfate groups can catalyze the degradation) as reported in Fig. 6c. Indeed, considering the proposed mechanisms and models (described earlier), amylose might play a role not only during hydrolysis but also in apparent particles size and plasticization. This is why a comparison of the different sources is proposed.

3.4. Influence of starch type

Differences between starches used for preparing SNC are: amylose/amylopectin ratio, intermediate material content, lipid content, amylose and amylopectin structure and interchain organization and crystalline types.

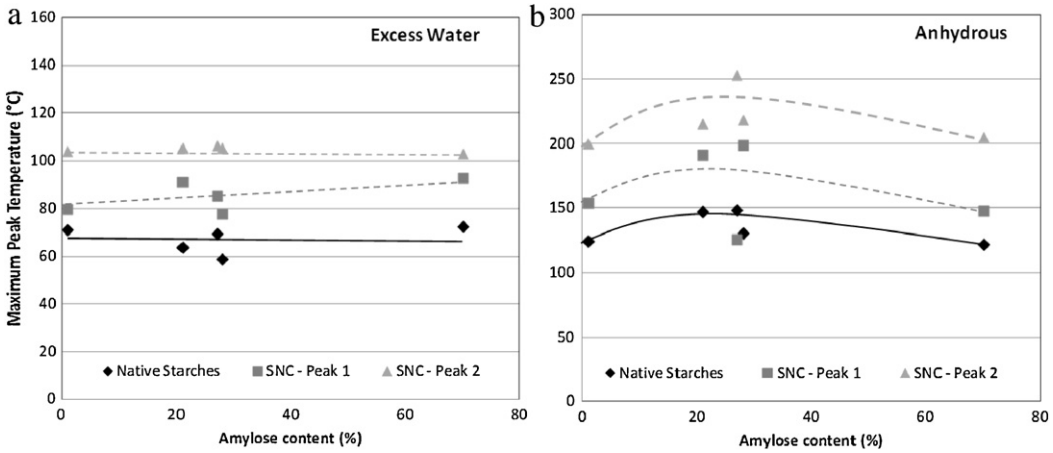

Fig. 5. Evolution of the endothermic peaks for native starch and freeze-dried SNC as a function of the initial amylose content in native starch (a) in excess water (70% water content) and (b) in the dry state (50% RH).

Table 2
Characteristic temperatures observed for the endothermic transitions of starches and corresponding SNC in excess water (starch:H_2O 30:70).

Starch type	WC (%)		Native				Nanocrystals							Comparison
			T_i (°C)	T_{max} (°C)	T_f (°C)	Range Δ (°C)	T_i (°C)	+/−	T_{max} (°C)	+/−	T_f (°C)	+/−	Range Δ (°C)	Shift of peak (°C)
M70	70	P1	69.1	72.5	78.3	9.2	84.5	12.5	93.0	2.1	99.9	1.0	15.4	20.5
		P2					106.7	6.3	103.1	3.5	112.9	5.2	6.2	
M27	70	P1	63.9	69.4	81.9	18.1	67.6	2.2	85.5	1.3	99.7	0.5	32.1	16.0
		P2					100.2	0.1	106.6	2.1	112.9	3.2	12.8	
M1	70	P1	65.0	71.4	83.4	18.4	54.5	14.9	79.7	11.6	99.2	0.3	44.7	8.3
		P2					99.9	0.5	104.0	1.6	108.6	0.8	8.6	
W28	70	P1	53.3	59.1	76.4	23.1	59.0	9.1	77.7	11.8	100.7	1.7	41.8	18.6
		P2					101.7	1.1	105.5	0.3	111.3	2.2	9.6	
P21	70	P1	59.6	64.0	82.5	22.9	82.1	10.2	91.3	4.3	100.3	0.5	18.2	27.3
		P2					101.6	0.4	105.5	0.1	110.0	1.6	8.4	

T_i: onset temperature; T_{max}: maximum peak temperature; T_f: final temperature; P1: first endothermic peak; P2: second.

Table 3
Characteristic temperatures observed for the endothermic transitions of starches and corresponding SNC in the dry state (50% RH conditioning).

Starch type	WC (%)		Native				Nanocrystals							Comparison
			T_i (°C)	T_{max} (°C)	T_f (°C)	Range Δ (°C)	T_i (°C)	+/−	T_{max} (°C)	+/−	T_f (°C)	+/−	Range Δ (°C)	Shift of peak (°C)
M70	0	P1	94.6	122.6	231.1	136.5	116.0	2.2	148.3	2.8	178.2	2.5	62.1	25.7
		P2					193.3	3.3	205.4	3.8	246.0	0.5	52.6	
M27	0	P1	109.6	148.7	255.0	145.4	105.0	7.8	126.1	6.3	161.0	0.2	56.0	−22.6
		P2					247.2	1.4	253.5	1.0	256.9	0.0	9.7	
M1	0	P1	107.6	124.7	223.5	115.9	123.4	11.2	154.0	2.2	180.3	10.2	56.9	29.3
		P2					188.0	9.1	200.0	10.2	234.0	7.4	46.0	
W28	0	P1	104.8	130.7	241.4	136.6	186.6	2.5	199.0	9.3	212.8	12.0	26.2	68.3
		P2					215.9	13.2	218.9	12.6	248.3	6.4	32.4	
P21	0	P1	111.6	147.6	204.8	93.2	178.9	3.0	191.4	9.2	205.4	23.1	26.4	43.8
		P2					207.0	21.7	215.3	9.7	245.5	5.6	38.4	

T_i: onset temperature; T_{max}: maximum peak temperature; T_f: final temperature; P1: first endothermic peak; P2: second endothermic peak.

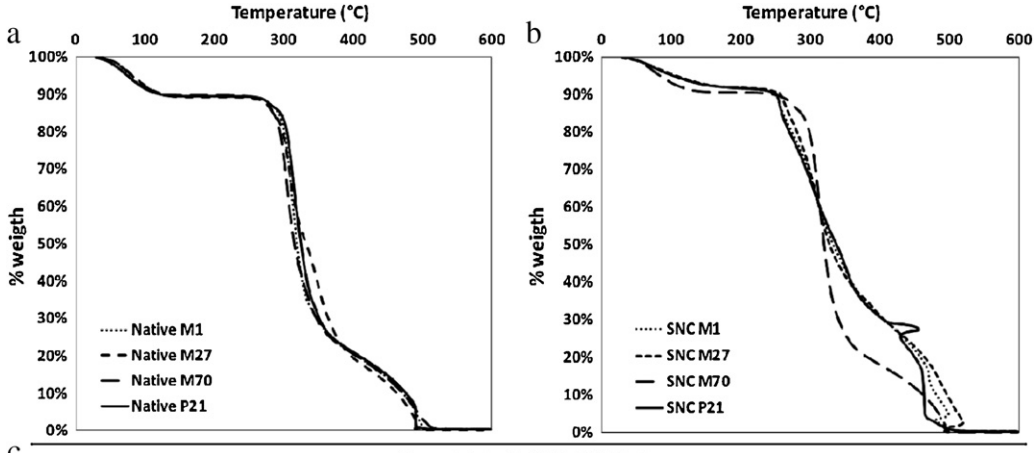

c

Temperature @ 15% weight loss			
	Native	SNC	Δ
M1	292	261	31
M27	286	268	18
M70	288	287	1
P21	286	262	24
W28	N.A.	N.A.	-

Fig. 6. TGA thermograms for (a) native starches and (b) corresponding SNC.

In excess water, differences among the first endothermic peak temperature (corresponding to the unpacking of double helices) of SNC from different crystalline types are observed. The results are presented in Table 2. In its native state, the B-type crystalline packing is described as less dense than A-type and hence more mobile and more prone to disruption (Luo, Fu, Gao, & Yu, 2011). Our results show opposite tendency. Indeed, for B-type starches SNC (M70 and P21) the first endothermic peak was shifted up to higher temperatures by 20–30 °C, whereas for A-type starches SNC the shift was below 20 °C (Table 2). Speculated explanation could be that (i) the amorphous backbone has been hydrolyzed and thus cannot exert pressure on the "less-densely organized" B-crystallites, and (ii) since B-type starches have longer amylopectin helixes, it induces a "rigidity effect" (Waigh, Gidley et al., 2000) which translates in the nematic state (i.e., out of lamellar order but still oriented) as opposed to an isotropic state. In the dry state on the contrary, the shift to higher temperatures is more important (up to 70 °C) as seen in Table 3. However, the second endothermic peak temperature (corresponding to the unwinding of helices) is the same for all SNC. No direct correlation between thermal transitions' temperature and initial amylose content was found as shown in Fig. 5a. Although, it seems for maize starch that the higher the amylose content, the higher the first endothermic peak temperature. This could be attributed to the fact that for maize starch, amylose content correlates with branch chain length; and thus the longer, the more rigid (as previously described) and the more stable.

In any case, the results also prove that SNC in excess water should not be processed at temperatures higher than 80 °C for wheat (W28) and waxy maize (M1) starches, 85 °C for normal maize starch (M27) and 90 °C for potato (P21) and high amylose (M70) starches. Indeed, if the integrity of the crystal is altered (by the opening up of the double helixes packing) then there is no point in using it as barrier material for example.

In dry conditions, no apparent correlation between thermal transitions' temperature and crystalline type or amylose content could be evidenced as seen in Fig. 5b. However, for maize starches, the two peaks were further apart than for wheat and potato starches, indicating that crystallites were less homogeneous.

Concerning degradation temperature, no influence of the starch source is observed for native starches as presented in Fig. 6a. For SNC, it could seem (Fig. 6b) that the higher the initial (and possibly residual) amylose content, the latter the onset for degradation. However, these data correlate better with SNC's diameter (Table 1) and thus with potential amount of sulfate groups at the surface as suggested before. These results show that, to a certain extent, SNC could be used in dry processing methods where temperature does not exceed 180 °C such as "cold" extrusion.

4. Conclusion

Investigation of the thermal properties of SNC from different sources by DSC revealed two thermal transitions, contrary to native starches which show only one transition. In excess water, the first peak was attributed to the first stage of crystallites melting (unpacking of the double helixes) and the second transition to the second stage of crystallites melting (unwinding of the helixes). B-type crystallinity SNC "gained" more stability than A-type SNC as they consist of more rigid crystallites. In the dry state, the peaks were attributed to crystallites melting, with a direct transition from packed helixes to unwinded helixes; and the presence of two peaks was attributed to heterogeneity in crystallites quality. It was demonstrated by TGA measurements that the second peak occurred before depolymerization and corresponded to the theoretical values of perfect crystallites melting. It confirms that SNC are individualized crystallites with small polymer chain length and high melting temperature. It has always been suspected that the type of starch used for preparing SNC was an important parameter. This study shows that the amylose content of starch shows little influence on final thermal properties of SNC. On the contrary, differences between starches observed in the native state are somewhat compensated when in SNC. However, it seems that in excess water B-type crystallites (with longer chain length) are more stable and that in dry conditions, maize SNC showed least homogeneous crystallites. Finally, it was proved that SNC can be used in wet processes, such as coating, if temperature remains lower than 80–100 °C, and in dry processes at temperatures below 150–200 °C.

Acknowledgments

The research leading to these results has received funding from the European Community's Seventh Framework Program (FP7/2007-2013) under grant agreement no. 207810.

References

Angellier, H. (2005). Nanocristaux d'amidon de maïs cireux pour applications composites. *Material sciences* (Vol. PhD thesis, p. 285). Grenoble, France: University Joseph Fourier.

Angellier, H., Choisnard, L., Molina-Boisseau, S., Ozil, P., & Dufresne, A. (2004). Optimization of the preparation of aqueous suspensions of waxy maize starch nanocrystals using a response surface methodology. *Biomacromolecules*, *5*, 1545–1551.

Angellier, H., Molina-Boisseau, S., Dole, P., & Dufresne, A. (2006). Thermoplastic starch–waxy maize starch nanocrystals nanocomposites. *Biomacromolecules*, *7*(2), 531–539.

Angellier, H., Molina-Boisseau, S., & Dufresne, A. (2005). Mechanical properties of waxy maize starch nanocrystal reinforced natural rubber. *Macromolecules*, *38*(22), 9161–9170.

Angellier, H., Molina-Boisseau, S., Lebrun, L., & Dufresne, A. (2005). Processing and structural properties of waxy maize starch nanocrystals reinforced natural rubber. *Macromolecules*, *38*(9), 3783–3792.

Angellier, H., Putaux, J.-L., Molina-Boisseau, S., Dupeyre, D., & Dufresne, A. (2005). Starch nanocrystal fillers in an acrylic polymer matrix. *Macromolecular Symposia*, *221*(1), 95–104.

Atichokudomchai, N., Varavinit, S., & Chinachoti, P. (2002). Gelatinization transitions of acid-modified tapioca starches by differential scanning calorimetry (DSC). *Stärke*, *54*(7), 296–302.

Barron, C. (1999). Destructuration d'amidons peu hydratés sous cisaillement. *ISITEM* (Vol. PhD, p. 164). Nantes: Université de Nantes.

Biliaderis, C. G. (2009). Structural transitions and related physical properties of starch. In J. B. Miller, & R. Whistler (Eds.), *Starch chemistry and technology* (pp. 293–372). Elsevier – Academic Press.

Biliaderis, C. G., Mazza, G., & Przybylski, R. (1993). Composition and physio-chemical properties of starch from cow cockle (*Saponaria vaccaria* L.) seeds. *Stärke*, *45*, 121–127.

Biliaderis, C. G., Page, C. M., Maurice, T. J., & Juliano, B. O. (1986). Thermal characterization of rice starches: A polymeric approach to phase transitions of granular starch. *Journal of Agricultural and Food Chemistry*, *34*(1), 6–14.

Biliaderis, C. G., Page, C. M., Slade, L., & Sirett, R. R. (1985). Thermal behavior of amylose–lipid complexes. *Carbohydrate Polymers*, *5*(5), 367–389.

Blanshard, J. M. V. (1987). Starch granule structure and function: A physicochemical approach. In T. Galliard (Ed.), *Starch: Properties and potentials* (pp. 16–54). London, UK: Society of Chemical Industry.

Chen, Y., Cao, X., Chang, P. R., & Huneault, M. A. (2008). Comparative study on the films of poly(vinyl alcohol)/pea starch nanocrystals and poly(vinyl alcohol)/native pea starch. *Carbohydrate Polymers*, *73*(1), 8–17.

Chen, G., Wei, M., Chen, J., Huang, J., Dufresne, A., & Chang, P. R. (2008). Simultaneous reinforcing and toughening: New nanocomposites of waterborne polyurethane filled with low loading level of starch nanocrystals. *Polymer*, *49*(7), 1860–1870.

Colonna, P., & Buleon, A. (2010). Thermal transitions of starches. In A. C. Bertolini (Ed.), *Starches: Characterization, properties, and applications* (pp. 71–102). NW: CRC Press.

Cooke, D., & Gidley, M. J. (1992). Loss of crystalline and molecular order during starch gelatinisation: Origin of the enthalpic transition. *Carbohydrate Research*, *227*, 103–112.

Donovan, J. W. (1979). Phase transitions of the starch–water system. *Biopolymers*, *18*, 263–275.

Dufresne, A., & Cavaillé, J.-Y. (1998). Clustering and percolation effects in microcrystalline starch-reinforced thermoplastic. *Journal of Polymer Science Part B: Polymer Physics*, *36*(12), 2211–2224.

Evans, I. D., & Haisman, D. R. (1982). The effect of solutes on gelatinization temperature range of potato starches. *Stärke*, *34*(7).

Garcia, N. L., Ribba, L., Dufresne, A., Aranguren, M. I., & Goyanes, S. (2009). Physicomechanical properties of biodegradable starch nanocomposites. *Macromolecule Materials and Engineering*, *294*(3), 169–177.

George, J., Ramana, K. V., Bawa, A. S., & Siddaramaiah. (2011). Bacterial cellulose nanocrystals exhibiting high thermal stability and their polymer nanocomposites. *International Journal of Biological Macromolecules*, *48*(1), 50–57.

Jiang, D. D., Yao, Q., McKinney, M. A., & Wilkie, C. A. (1999). TGA/FTIR studies on the thermal degradation of some polymeric sulfonic and phosphonic acids and their sodium salts. *Polymer Degradation and Stability*, *63*, 423–434.

Kasemsuwan, T., & Jane, J. (1994). Location of amylose in normal starch granules. II. Locations of phosphodiesterase cross-linking revealed by phosphorus-31 nuclear magnetic resonance. *Cereal Chemistry*, *71*, 282–287.

Kristo, E., & Biliaderis, C. G. (2007). Physical properties of starch nanocrystal-reinforced pullulan films. *Carbohydrate Polymers*, *68*(1), 146–158.

Le Corre, D., Bras, J., & Dufresne, A. (2010). Starch nanoparticles: A review. *Biomacromolecules*, *11*(5), 1139–1153.

LeCorre, D., Bras, J., & Dufresne, A. (unpublished results). Influence of botanic origin and amylose content on the morphology of starch nanocrystals. *Journal of Nanoparticle Research*.

Lin, N., Huang, J., Chang, P. R., Anderson, D. P., & Yu, J. (2011). Preparation, modification and application of starch nanocrystals in nanomaterials: A review. *Journal of Nanomaterials*, *2011*, 13.

Luo, Z.-g., Fu, X., Gao, Q.-y., & Yu, S.-J. (2011). Effect of acid hydrolysis in the presence of anhydrous alcohols on the structure, thermal and pasting properties of normal, waxy and high amylose maize starches. *International Journal of Food Science & Technology*, *46*, 429–435.

Ma, X., Chang, P. R., Yu, J., & Stumborg, M. (2009). Properties of biodegradable citric acid-modified granular starch/thermoplastic pea starch composites. *Carbohydrate Polymers*, *75*(1), 1–8.

Oates, C. G. (1997). Towards an understanding of starch granule structure and hydrolysis. *Trends in Food Science & Technology*, *8*(11), 375–382.

Randzio, S. a. L., Flis-Kabulska, I., & Grolier, J.-P. E. (2002). Reexamination of phase transformations in the starchâ' water system. *Macromolecules*, *35*(23), 8852–8859.

Roman, M., & Winter, W. T. (2004). Effect of sulfate groups from sulfuric acid hydrolysis on the thermal degradation behavior of bacterial cellulose. *Biomacromolecules*, *5*(5), 1671–1677.

Salam, A., Pawlak, J. J., Venditti, R. A., & El-tahlawy, K. (2010). Synthesis and characterization of starch citrateâ' chitosan foam with superior water and saline absorbance properties. *Biomacromolecules*, *11*(6), 1453–1459.

Tester, R. F., & Morrison, W. R. (1990). Swelling and gelatinization of cereal starches. I. Effects of amylopectin, amylose, and lipids. *Cereal Chemistry*, *67*, 551–557.

Tester, R. F., & Morrison, W. R. (1992). Swelling and gelatinization of cereal starches. III. Some properties of waxy and normal nonwaxy barley starches. *Cereal Chemistry*, *69*(6), 654–658.

Thielemans, W., Belgacem, M. N., & Dufresne, A. (2006). Starch nanocrystals with large chain surface modifications. *Langmuir*, *22*(10), 4804–4810.

Viguié, J., Molina-Boisseau, S., & Dufresne, A. (2007). Processing and characterization of waxy maize starch films plasticized by sorbitol and reinforced with starch nanocrystals. *Macromolecular Bioscience*, *7*(11), 1206–1216.

Waigh, T. A., Gidley, M. J., Komanshek, B. U., & Donald, A. M. (2000). The phase transformations in starch during gelatinisation: A liquid crystalline approach. *Carbohydrate Research*, *328*(2), 165–176.

Waigh, T. A., Kato, K. L., Donald, A. M., Gidley, M. J., Clarke, C. J., & Riekel, C. (2000). Side-chain liquid-crystalline model for starch. *Stärke*, *52*(12), 450–460.

Wang, N., Ding, E., & Cheng, R. (2007). Thermal degradation behaviors of spherical cellulose nanocrystals with sulfate groups. *Polymer*, *48*(12), 3486–3493.

Whistler, R. L., & BeMiller, J. (2009). *Starch: Chemistry and technology*. New York: Elsevier.

Yu, J., Ai, F., Dufresne, A., Gao, S., Huang, J., & Chang, P. R. (2008). Structure and mechanical properties of poly(lactic acid) filled with (starch nanocrystal)-graft-poly(e-caprolactone). *Macromolecule Materials and Engineering*, *293*(9), 763–770.

Zheng, H., Ai, F., Chang, P. R., Huang, J., & Dufresne, A. (2009). Structure and properties of starch nanocrystal-reinforced soy protein plastics. *Polymer Composites*, *30*(4), 474–480.

Zhong, Z., & Sun, X. S. (2005). Thermal characterization and phase behavior of cornstarch studied by differential scanning calorimetry. *Journal of Food Engineering*, *69*(4), 453–459.